Textile & Leather Review

ISSN 2623-6281 | www.tlr-journal.com | 10.31881/TLR

Extraction of Cellulose Nanocrystals from Nypa fruticans and Their Reinforcement Effect in PVC–Leather Waste Composites

Md. Ariful Islam, Nujhat Tabassum, Md. Abdus Shabur, Umme Habiba Bodrun Naher, Md. Abdul Mottalib

How to cite: Islam M, Tabassum N, Shabur M, Naher U, Mottalib M. Extraction of Cellulose Nanocrystals from Nypa fruticans and Their Reinforcement Effect in PVC–Leather Waste Composites. Textile & Leather Review. 2026; 9:6039-6067. https://doi.org/10.31881/TLR.2026.6039

How to link: https://doi.org/10.31881/TLR.2026.6039

Published: 5 June 2026

Extraction of Cellulose Nanocrystals from Nypa fruticans and Their Reinforcement Effect in PVC–Leather Waste Composites

Md. Ariful Islam[1], Nujhat Tabassum[1], Md. Abdus Shabur[1,2], Umme Habiba Bodrun Naher[1], Md. Abdul Mottalib[1*]

[1]Institute of Leather Engineering and Technology, University of Dhaka, Dhaka-1209, Bangladesh

[2]King Fahd University of Petroleum and Minerals (KFUPM), Dhahran, 31261, Kingdom of Saudi Arabia

*abdul.mottalib@du.ac.bd

Article

https://doi.org/10.31881/TLR.2026.6039

Published 5 June 2026

ABSTRACT

The growing generation of leather waste poses severe environmental challenges, demanding sustainable valorization strategies. This study presents an innovative approach to developing high-performance composites by extracting cellulose nanocrystals (CNC) from Nypa fruticans, a locally abundant mangrove biomass, and integrating them into PVC–leather scrap matrices reinforced with Al2O3. CNC was obtained via oxidation, yielding nanocrystals with a diameter of ~100 nm and 78.07% crystallinity, as confirmed by FTIR, XRD, FESEM, and DLS analyses. Composite sheets were fabricated with optimized CNC loadings (1–4 %) and evaluated for mechanical, thermal, and moisture-resistance properties. The hybrid composite containing 3 % CNC and 4 % Al2O3 exhibited improved performance, achieving a tensile strength of 3.43±0.14 Nmm^{-2}, an enhancement of about 120% compared to the control, and an elongation at break of 25.13±1.11%. Thermogravimetric analysis showed improved thermal stability, with a degradation onset near 380 °C and an increased char yield (5.09 % vs. 1.02 % for the control). Water absorption decreased to 19.63 %, indicating enhanced compactness and interfacial bonding. The study establishes Nypa fruticans as a novel, renewable feedstock for CNC production and demonstrates a synergistic reinforcement effect between bio-derived CNC and inorganic Al2O3 within the PVC–leather matrix. These results contribute to the theoretical understanding of structure–property relationships in hybrid nanocomposites and offer a scalable, eco-efficient route for transforming industrial leather waste into functional materials. The developed composites exhibit strong potential for use in footwear, insole boards, and leather goods, aligning with circular-economy and sustainable-manufacturing objectives.

KEYWORDS

bio-composite, cnc, waste-upcycling, leather scrap, sustainable materials

INTRODUCTION

Leather has long played a crucial role in shaping the identity and aesthetics of the fashion industry, being traditionally valued for its luxurious texture, durability, and versatility in clothing, accessories, and footwear. However, the very attributes that make leather desirable also raise concerns regarding its environmental footprint [1]. About 80-85% of solid waste is generated during hide processing [2], whereas 20-25% of finished leather scraps are generated in footwear manufacturing, resulting in considerable ecological impacts [3]. Tannery solid waste poses a significant environmental threat, as it often contains hazardous chemicals such as chromium and sulfides that can contaminate soil, water, and air, leading to severe ecological degradation if not disposed of properly. While some of this waste is recycled or repurposed, a significant portion still ends up in landfills or is incinerated, contributing to air pollution and further environmental degradation. Recognizing these challenges, researchers have introduced strategies to minimize the sector's environmental impacts, emphasizing cleaner production practices and effective waste reduction in tanneries. A promising solution lies in adopting circular economy (CE) principles, which encourage recycling, reuse, and upcycling, such as transforming discarded footwear into new products. Such measures would help reduce dependence on virgin raw materials while minimizing environmentally damaging disposal practices. The integration of CE practices into industrial sectors has become increasingly essential to achieving the Sustainable Development Goals (SDGs) globally. Despite the potential benefits of CE in reducing environmental impacts and recovering value from waste, its implementation in the leather sector remains limited and challenging [4]. Waste reduction strategies-such as improving production efficiency, promoting repair and refurbishment, and fostering a culture of reuse - are therefore critical to mitigating the industry's environmental footprint [5]. Leather waste, a major byproduct of the global leather industry, poses serious environmental challenges due to its high organic load, resistance to degradation, and potential to pollute. Converting this waste into highly value-added products, particularly bio-composites, offers a promising CE strategy that reduces ecological burdens while creating advanced functional materials [6].

Against this backdrop, valorizing leather waste through the incorporation of nanocellulose represents a forward-thinking convergence of waste management, materials science, and sustainable innovation. Nanocellulose, derived from renewable sources such as wood, plants, agricultural residues, or bacterial synthesis, has garnered significant attention due to its unique properties, including high tensile strength, biodegradability, and large surface area [7]. These attributes make it an excellent reinforcement material for polymer and bio-

based composites, with demonstrated benefits in mechanical strength, thermal stability, and environmental performance. When integrated with leather waste, nanocellulose acts as a structural enhancer, producing lightweight, durable, and sustainable composites [8]. Such bio-nanocomposites hold potential applications in synthetic leather alternatives, shoe insole boards, automotive interiors, and construction panels. Life cycle assessment (LCA) studies have also confirmed reduced energy consumption and greenhouse gas emissions compared to traditional polyurethane-based products [9]. Composite materials derived from natural fibers have attracted widespread attention and are used in diverse applications, including electrical appliances, packaging, building and construction reinforcement, and automobile interior components [10]. Advancements in bio-fiber production have enabled the development of high-performance composite materials, as these fibers can be processed into micro- or nanoscale fibers with enhanced mechanical strength and increased surface area [11].

Building on this foundation, a recent study extracted cellulose nanocrystals (CNCs) from Slender amaranth - a commonly discarded vegetable waste and incorporated them into leather scrap-based composites using isoprene rubber latex as a binder [12]. The results showed significant improvements that outperformed many earlier-reported materials, underscoring the potential of combining leather-industry waste with plant-derived nanomaterials to create high-performance, low-cost, and sustainable alternatives for shoe uppers and other leather goods [13]. The fabrication of composite materials from leather solid waste, combined with plant fibers derived from cellulose and nanocellulose, offers a cost-effective and eco-friendly approach that minimizes environmental pollution while producing materials with improved mechanical properties [14]. Basalt fibers have emerged as effective reinforcement materials for composite fabrication [15]. Jute fiber, obtained from the jute plant, is also considered a highly promising material for composite applications [16]. Additionally, reconstituted composites can be produced by blending discarded leather fibers with cotton and polyester fibers [17,18].

The Nipa palm (*Nypa fruticans*) is a key mangrove species in Bangladesh's coastal regions. This tree is available in Bangladesh and grows readily under local environmental conditions. To our knowledge, no study has been published on the extraction of cellulose nanocrystals (CNC) from *Nypa fruticans* waste and their use in the manufacturing of leather-based biocomposites. CNC extraction and characterization of this underutilized biomass, and its incorporation into leather scrap waste bio-composite sheets with PVC as a binder, are unique. Finished leather waste accounts for the majority of solid leather discards in the footwear industry. Turning

this waste into useful, value-added composites reduces environmental impact and creates economic opportunities. To fill this gap, this project will create leather-based composite sheets reinforced with CNC from *Nypa fruticans* fibers and assess their mechanical, thermal, and physical properties. Advanced analytical methods were used to characterize the shape, crystallinity, and functional groups of the isolated nanocellulose fibers. The study also suggests using bio-derived nanofibers as sustainable reinforcement materials in PVC-based leather composites for shoe upper leather and leather goods manufacturing. By reducing waste and creating jobs, this technique reduces environmental impact and improves sustainability.

Research Gap and Novelty of the Current Study

Many studies have examined recovering leather waste and making bio-based composites; however, there are still important gaps in material design and sustainability integration. Most of the work done so far uses natural fibers such as jute, kenaf, or banana as reinforcements. These fibers are usually only valid on a small scale and don't link well with polymers or spread out nicely in polymer matrices. Also, the extraction of cellulose nanocrystals (CNCs) has mostly come from traditional sources like wood pulp or crop leftovers. This means that many lignocellulosic biomasses that are common in some areas have not been studied enough. *Nypa fruticans*, a readily accessible mangrove species in coastal Bangladesh, has not been documented as a source for CNC extraction, despite its significant cellulose production potential. In a similar vein, while leather solid waste has been transformed into composites, the application of polyvinyl chloride (PVC) as a binder, alongside nanocellulose reinforcement, remains underexplored. Furthermore, the synergistic effects of inorganic fillers, such as Al_2O_3 , on enhancing the structural and thermal properties of these composites have yet to be thoroughly investigated.

To address these knowledge deficiencies, the current study presents an innovative and sustainable method for fabricating high-performance composites by extracting cellulose nanocrystals (CNCs) from *Nypa fruticans* and integrating them into PVC-leather scrap matrices, supplemented with Al_2O_3 as an inorganic filler. This dual-reinforcement method uses both bio-derived and inorganic nanofillers to make materials stronger, more heat- and water-resistant, and generate less waste. The research presents the inaugural extensive characterisation of *Nypa fruticans*–derived CNCs, employing advanced analytical methodologies, and links their nanoscale attributes to macroscopic composite characteristics. This work adds both scientific novelty and practical relevance within the framework of the circular economy and sustainable material innovation by valorizing two waste resources, such as plant biomass and leather scraps, into useful materials appropriate for footwear and

leather items. The main objective of the study was to extract and characterize cellulose nanocrystals (CNCs) from *Nypa fruticans* using chemical treatment and oxidation processes, and to fabricate PVC–leather waste composite sheets reinforced with CNCs and inorganic fillers (Al_2O_3), optimizing composition and processing c onditions to achieve improved mechanical and thermal performance.

MATERIALS AND METHODS

Materials

Nypa fruticans leaves were collected from the mangrove forests of the Sundarbans, Bangladesh, and used as a source of cellulose. Scrap leather waste was obtained from Leather Industry Bangladesh (LIB), Hazaribagh, Dhaka, and processed into fibers for composite preparation. Analytical-grade chemicals such as NaOH pellets, $NaClO_2$, H_2O_2 , $NaNO_2$, HNO_3 , $CaCO_3$, Al_2O_3 , ZnO, PVC, and THF were used throughout the study, purchased from Merck, India.

Cellulose extraction

Alkali-treated fiber preparation

The *Nypa fruticans* leaves were separated from the midribs and cut into small pieces approximately 3–4 inches long. The leaf pieces were thoroughly washed with tap water to remove dirt, dust, and other surface impurities, then rinsed with distilled water and sun-dried for 2 days. The dried leaves were then ground into a fine powder to increase surface area and facilitate extraction. The powdered leaves were subjected to alkali treatment with 5% and 10% NaOH solutions separately for 24 hours, maintaining a leaf-to-liquor ratio of 1:20 at room temperature. After treatment, the suspensions were sieved to separate the treated fibers, which were repeatedly rinsed with distilled water to remove residual alkali. The treated fibers were then oven-dried at 60 °C for 24 hours.

Bleaching treatment

The alkali-treated fibers were bleached in 2% sodium chlorite ($NaClO_2$)at 100 °C for 6 hours, changing color fr om dark to light brown. They were filtered, washed with distilled water until neutral pH, and oven-dried at 6 0 °C for 24 hours.

To achieve further delignification and improved structural properties, the partially bleached fibers underwent a secondary bleaching step using hydrogen peroxide (H_2O_2). The fibers were treated with a 2% H_2O_2 solution at 100 °C for 6 hours, resulting in a color change from light brown to white. After bleaching, the fibers

were again filtered, washed repeatedly to remove residual chemicals and neutralize the pH, and dried at 60 °C for 24 hours. The final product obtained was purified cellulose.

Nano-cellulose preparation

5 g dried cellulose was placed in a round-bottom flask and dispersed in 25 mL of distilled water. A 64% nitric acid (HNO_3) solution was then prepared separately by gradual dilution and slowly added to the cellulose dispersion under continuous stirring. Subsequently, sodium nitrite ($NaNO_2$) was introduced at a 1:1 (w/w) ratio relative to cellulose, initiating nitration and oxidation and releasing red fumes (NOx gases). The reaction was carried out under reflux conditions using a condenser in a fume hood to ensure controlled reaction conditions and safe handling of gaseous byproducts. The reaction was maintained at 60 °C for discrete reaction times of 10, 12, 14, and 16 hours (to evaluate the effect of reaction duration) under constant stirring at 1,000 rpm. After completion, the reaction mixture was quenched with 300 mL of cold distilled water, and the resulting precipitate was repeatedly washed and centrifuged until the pH was neutral. The purified suspension was then preserved in ethanol and stored at 4 °C for subsequent use as nanocellulose [19]. The extraction processes are shown in Figure 1.

Figure 1. Process flow diagram of cellulose preparation

Effect of reaction time on nanocellulose extraction

To optimize the reaction time for nanocellulose extraction, four trials were conducted by varying the reaction time while keeping the other parameters constant as per the literature [19] (Table 1). The reaction times were

set to 10, 12, 14, and 16 hours, respectively. This optimization allowed assessment of the influence of reaction duration on nanocellulose formation. It should be noted that yield was not evaluated in this study, as the primary focus was on investigating the effect of reaction time on nanocellulose size.

Table 1. Effect of reaction time on nanocellulose preparation

Expt. No.	Cellulose:$NaNO_2$ ratio (w/w)	HNO_3 concentration	Temperature (°C)	Reaction time (h)
1	1:1	64	60	10
2	1:1	64	60	12
3	1:1	64	60	14
4	1:1	64	60	16

Composite preparation

Leather fibers (LF) were prepared from scraps collected from Leather Industry Bangladesh (LIB), a footwear industry. The scraps were cut into small pieces (1–2 cm in length and 0.5–1 cm in width), washed twice, and dried in an oven at 110 °C for 2h. The dried pieces were then converted into fibers using a crushing machine. For composite fabrication, the leather fibers were soaked in water for 2–3 hours and manually minced to enhance flexibility and surface activity. The excess water was then removed by manual pressing using a mesh to obtain a moist but not water-saturated fiber structure. Polyvinyl chloride (PVC) was selected as the binder for its strong adhesion and flexibility, and ethylene glycol served as the plasticizer. Calcium carbonate ($CaCO_3$), aluminum oxide (Al_2O_3), and zinc oxide (ZnO) were incorporated as inorganic fllers to improve co mposite strength and stability. PVC was first dissolved in tetrahydrofuran (THF) to form a homogeneous so lution. This solution was then applied to the pre-pressed leather fiber along with the fillers and plasticizer, al lowing the polymer to infiltrate and coat the fiber network. The moist sheet was initially compressed for 10 se conds using a hydraulic press at 1500 psi. After drying under sunlight for 1-2 days, the sheets were further pl ated using a hydraulic press at 2000 psi and 70 °C for 10 seconds, yielding the final composite material. The d etailed composition of each formulation is presented in Table 2.

Table 2. Composition of control composite formulation

Sample Id	Leather fiber (%)	PVC (%)	Ethylene glycol (% with respect to PVC)
S1	25	75	4
S2	30	70	4
S3	33.33	66.67	4
S4	35	65	4
S5	40	60	4

Among all the tested formulations, the best mechanical performance was observed for S3, where the incorporation of inorganic fillers further enhanced the material's overall strength, durability, and stability (Table 3).

Table 3. Composition including inorganic fillers

Sample Id	Leather fiber (%)	PVC (%)	Ethylene glycol (% with respect to PVC)	Filler (% of Al_2O_3)
S31	33.33	66.67	4	4% of Al_2O_3
S32	33.33	66.67	4	4% $CaCO_3$
S33	33.33	66.67	4	4% ZnO

Based on the mechanical test performance results, Al_2O_3 was selected as the preferred filler. Nanocellulose was subsequently incorporated into this composition, and further analyses were carried out.

Nano-cellulose-incorporated composite preparation

The preparation of nanocellulose-based scrap leather composites involved additional steps in which nanocellulose was incorporated to reinforce the matrix and improve the material's overall mechanical performance. Nanocellulose was extracted from *Nypa fruticans* leaves using the chemical treatment method described earlier. The extracted nanocellulose was finely dispersed in distilled water using an ultrasonicator, then added to the composite mixture.

The nanocellulose was incorporated into the leather fiber–PVC matrix in varying proportions (relative to leather fiber), as summarized in Table 4. To ensure uniform dispersion, the mixtures were sonicated before compounding. After mixing the leather fibers, PVC binder, inorganic fillers, and nanocellulose, the blended mass was compounded under pressure to achieve a homogeneous structure. The slurry was poured into molds and manually pressed to remove excess water. The resulting wet sheets were compressed for 10 seconds under 1500 psi using a hydraulic press. After sun drying for 1–2 days, the sheets were subjected to a final pressing at 2000 psi and 70 °C for 10 seconds, yielding fully cured nanocellulose-incorporated composites.

Table 4. CNC-incorporated composite formulation

Sample Id	Leather fiber (%)	PVC (%)	Ethylene glycol (% with respect to PVC)	Filler (% of Al_2O_3)	Nano-cellulose (%)
S311	33.33	66.67	4	4	1
S312	33.33	66.67	4	4	3
S313	33.33	66.67	4	4	4

Characterization techniques

Fourier Transform Infrared (FTIR) spectroscopy

Fourier Transform Infrared (FTIR) spectroscopy was carried out on the prepared composites using a BRUKER ALPHA II FTIR spectrometer equipped with a single ATR reflection unit. Spectra were recorded in the range of 4000–450 cm^{-1} with a resolution of 4 cm^{-1}. The obtained spectra were analyzed to identify characteristic functional groups and to compare the chemical features of cellulose, nanocellulose, and the composite materials.

Thermo Gravimetric Analysis (TGA)

Thermogravimetric Analysis (TGA) was performed using a PerkinElmer TGA-8000 instrument under a nitrogen atmosphere to observe the stability of the composite samples. The samples were heated from 50 to 700 °C at 10 °C/min, with a constant nitrogen purge of 20 mL/min. The recorded weight loss as a function of temperature was used to evaluate the thermal stability and decomposition behavior of the composite materials.

X-ray Diffraction (XRD) analysis

X-ray Diffraction (XRD) analysis was performed using a Rigaku Ultima IV diffractometer, operated at 40 kV and 30 mA. Diffraction patterns were collected over a 2θ range of 10–70°, and the obtained data were analyzed to determine the crystal structure, identify specific crystallographic phases, and evaluate their relative abundance within the composite material.

Field Emission Scanning Electron Microscopy (FESEM)

Field-Emission Scanning Electron Microscopy (FESEM) was conducted to examine the surface morphology and microstructural characteristics of the composite material. Samples were sputter-coated with a thin platinum layer to ensure conductivity and imaged using a JOEL JSM-7610F field-emission scanning electron microscope operated at 5 kV. High-resolution images at different magnifications provided detailed insights into the surface

features and microstructural arrangement, contributing to a better understanding of the composite's performance and potential applications.

Dynamic Light Scattering (DLS)

Dynamic Light Scattering (DLS) analysis was carried out to determine the particle size distribution of the prepared nanocellulose using a Litesizer 500 Particle Analyzer (Anton Paar, Austria). The instrument was equipped with a 658 nm laser as the light source. Measurements were performed in aqueous suspension, where fluctuations in the intensity of scattered light caused by the Brownian motion of nanoparticles were recorded. The hydrodynamic diameter and size distribution were calculated using the Stokes–Einstein equation. DLS analysis provided valuable insights into the dispersion quality, particle size range, and stability of the nanocellulose suspension, which are critical parameters for composite reinforcement applications.

Mechanical assessment

The tensile strength and elongation at break of the composite materials were evaluated using a Universal Testing Machine (UTM) [Model No. STM 566 Tensile Tester] in accordance with the SATRA TM 137 standard. Rectangular specimens with dimensions of 110 mm × 25 mm and a gauge length of 50 mm were prepared using a precision cutting method. Each specimen was clamped securely in the UTM jaws, with an initial jaw separation of 20 mm, and subjected to a uniaxial tensile load at a constant crosshead speed of 100 mm/min until failure. During the test, the applied load and displacement were continuously monitored, and the data were recorded for analysis. Tensile strength (N/mm²) was determined by dividing the maximum load at failure by the initial cross-sectional area of the specimen. All mechanical tests were performed in triplicate (n = 3), and the results are reported as mean ± standard deviation.

Water absorption

The water-absorption behavior of the composite materials was evaluated according to ASTM D570. Rectangular specimens (1 × 1 inch) were prepared following the standard sample preparation procedure and immersed in 250 mL of distilled water at room temperature for 8 hours. After immersion, the samples were carefully removed, and surface water was gently blotted before weighing. The percentage of water absorption was calculated using the formula:

Percentage (%) of water absorption of the sample = $(M/M_1) \times 100$

where $M = M_2 - M_1$, M_2 is the wet weight of the sample after immersion, and M_1 is the initial dry weight of the sample.

RESULTS AND DISCUSSION

Characterization of CNC fibers

Fourier Transform Infrared (FTIR) spectroscopy analysis

Figure 2 shows the FTIR spectra of raw *Nypa fruticans* fibers, alkali-treated fibers, extracted cellulose, and the prepared cellulose nanocrystals. The spectra highlight the main absorption bands of cellulose, hemicellulose, and lignin in the raw fiber. The broad O–H stretching band at ~3331 cm^{-1} and C–H stretching at ~2917 cm^{-1} indicate hydroxyl groups and aliphatic C–H bonds. The distinct carbonyl peak at 1726 cm^{-1} is attributed to C=O stretching vibrations from hemicellulose and lignin. Specific aromatic C=C stretching at 1630 cm^{-1}, along with peaks at 1442, 1373, and 1231 cm^{-1}, further confirms the presence of non-cellulosic components [20]. Strong absorptions at ~1044 cm^{-1} correspond to C–OH stretching in cellulose and hemicellulose. The band at 803 cm^{-1} reflects aromatic C–H out-of-plane bending typical of lignin. After alkali treatment, significant reductions in the O–H, C=O, and lignin-associated peaks were observed. This demonstrates the progressive removal of hemicellulose and lignin [21]. The spectra of fibers after bleaching showed notable changes, confirming further purification of cellulose. The sharpening of the carbonyl peak at 1726 cm^{-1} suggests oxidation of hydroxyl groups into carbonyl groups during acid treatment. Cellulose-related peaks became more prominent. The CH_2 bending vibration at 1426 cm^{-1} and the β(1,4)-glycosidic linkage at 897 cm^{-1} were intensified. This suggests that cellulose became the dominant component as hemicellulose and lignin were progressively eliminated [19].

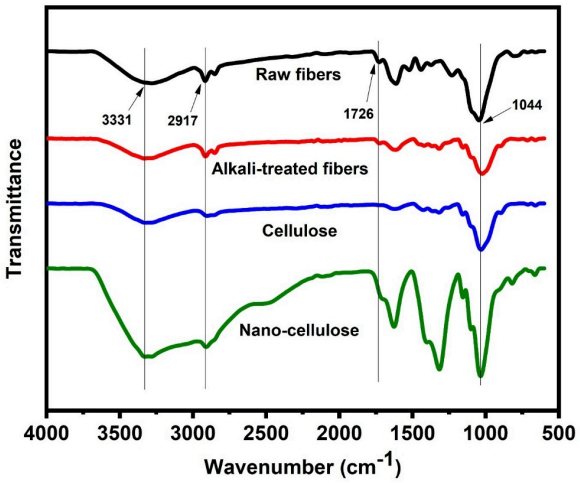

Figure 2. FTIR spectra of raw fiber, alkali-treated fiber, extracted cellulose, and nanocellulose

The FTIR spectrum of the prepared nanocellulose confirms both the preservation of cellulose functionalities and the introduction of new groups during oxidation. The O–H stretching band at ~3328 cm^{-1} reflects the abundance of surface hydroxyl groups responsible for hydrogen bonding, while the C–H stretching at 2911 cm^{-1} corresponds to the polysaccharide backbone. Hemicellulose and lignin exhibit C=O stretching at 1732 cm^{-1}, indicating the introduction of carboxyl groups, which enhance surface reactivity and interfacial bonding [22]. In the nanocellulose FTIR spectrum, a dominant peak was observed at 1635 cm^{-1} due to the O–H bending vibration of absorbed water molecules, which is commonly observed in cellulose due to its hygroscopic nature [23].

Other important features include CH_2 bending at 1402 cm^{-1}, C–O stretching at 1316 and 1034 cm^{-1}, and the β(1,4)-glycosidic C–O–C stretching at 820 cm^{-1}, which together confirm the crystalline cellulose structure of the nanomaterial. FTIR analysis confirmed the progressive transformation of *Nypa fruticans* fibers, where alkali and bleaching removed hemicellulose and lignin, enriching cellulose, while oxidation introduced carboxyl groups into nanocellulose, as shown by the absence of the 1732 cm^{-1} peaks in Figure 2 [24]. These modifications validate successful purification and functionalization, enhancing its potential as a reinforcing material without compromising the cellulose backbone. The chemical reactions of cellulose with alkali are shown below:

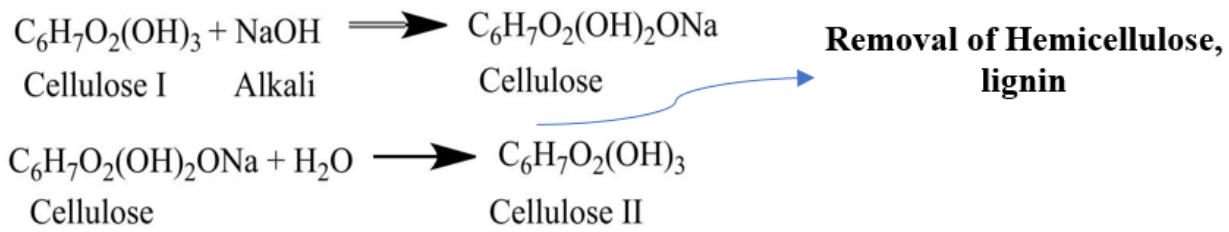

Dynamic Light Scattering (DLS) analysis

The extraction of nanocellulose from agricultural waste is important because it turns waste into a valuable, high-performance material, provides a renewable substitute for petroleum-based products, and opens new economic opportunities through advanced materials for industries such as construction, packaging, biocomposites, and healthcare. This method uses a lot of biomass resources, reduces environmental pollution, and leverages the unique properties of nanocellulose, such as its remarkable strength, biodegradability, and biocompatibility. Dynamic Light Scattering (DLS) analysis was performed to evaluate the particle size evolution of nanocellulose produced through oxidation, and the results are shown in Figure 3.

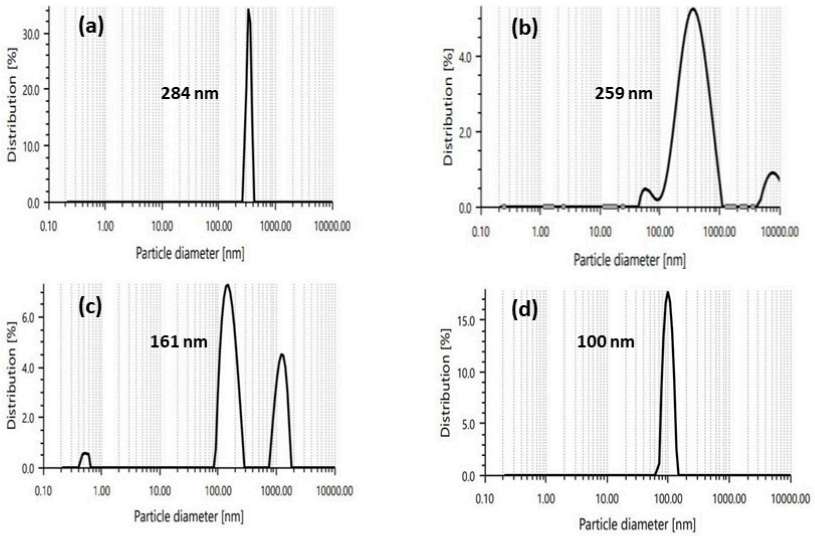

Figure 3. CNC size distribution profiles for reaction time (a) 10 h, (b) 12 h, (c) 14 h, and (d) 16 h

The results reveal a distinct trend of progressive size reduction with increasing reaction time under a fixed acid concentration. At 10 hours of reaction time, the average particle size was 284 nm. To obtain the expected nanoparticle size, experiments were conducted at different reaction times. Extending the reaction time led to a gradual decrease in particle size, with 259 nm observed at 12 hours, whereas 161 nm was observed at 14 hours. Finally, the cellulose size was found to be 100 nm after 16 hours under the same reaction conditions. This continuous reduction confirms that prolonged nitric acid oxidation effectively reduces cellulose fibers to nanoscale dimensions by cleaving amorphous regions and facilitating fibrillation. The final particle size of ~100 nm is particularly significant for nanocellulose applications. A smaller particle size corresponds to a higher surface area-to-volume ratio, which enhances interfacial interactions between nanocellulose and the host matrix. This increased surface activity improves filler dispersion, promotes stronger interfacial adhesion, and enables more efficient stress transfer across the composite interface [25]. As a result, nanocellulose at this scale is expected to impart superior mechanical reinforcement, improved thermal stability, and better compatibility with polymeric or inorganic matrices. Therefore, the DLS findings not only verify the successful synthesis of nanoscale cellulose but also underscore its potential as a high-performance reinforcing phase in bio-based composite systems [26].

Composite characterization

FTIR analysis

All spectra of the composites (Figure 4) exhibited a broad O–H stretching band near 3310 cm^{-1}, attributed to the hydroxyl groups present in both leather fibers and CNC. The characteristic C–H stretching vibration of the PVC backbone was clearly observed at 2917 cm^{-1}, while a distinct peak around 1632 cm^{-1} corresponded to the amide I band (C=O stretching) of collagen in leather [27]. It is also considered for the aromatic ring. Additionally, a sharp absorption band near 696 cm^{-1} confirmed the presence of PVC through C–Cl stretching vibrations, further validating the retention of the polymer structure in the composites. Upon the incorporation of fillers, notable spectral variations were detected. In the Al_2O_3 containing composite, the band at 1058 cm^{-1} became more intense, suggesting overlapping contributions from Al–O bonds and C–O stretching vibrations, which is indicative of strong interfacial interactions between the inorganic filler and the polymer matrix. For the $Al_2O_3 - CNC$ reinforced composite, further spectral changes were observed: the O–H band broadened and increased in intensity, while the band at 1058 cm^{-1} became sharper and more defined. These modifications can be attributed to enhanced C–O–C and C–O stretching vibrations originating from cellulose nanocrystals, thereby confirming their active participation in the composite structure [28]. These spectral shifts not only validate the successful incorporation of Al_2O_3 and CNC into the PVC–leather matrix but also highlight the synergistic interactions among fillers, fibers, and the polymer. Such interfacial compatibility is crucial, as it directly contributes to the improved dispersion of fillers and, consequently, to the enhanced mechanical, thermal, and structural properties of the developed composites.

In summary, the FTIR analysis—progressing from untreated *Nypa fruticans* fibers through alkali/bleached treatments, nanocellulose extraction, and finally composite formation demonstrates a clear chemical transformation at each stage. The removal of hemicellulose and lignin, the preservation and functionalization of cellulose, and the establishment of strong interactions between fillers and the PVC matrix all point toward enhanced structural integrity.

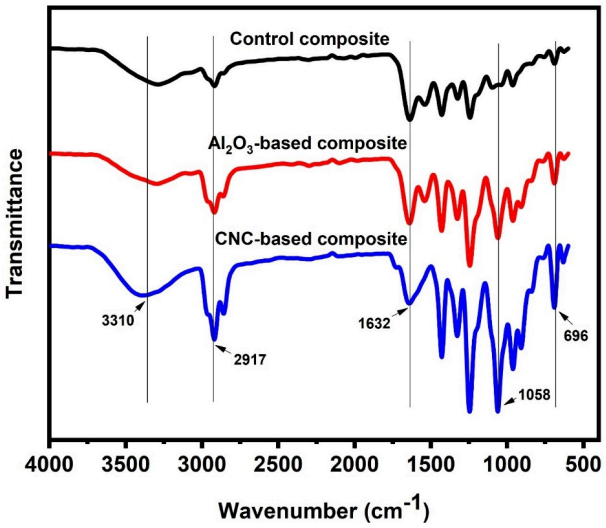

Figure 4. FTIR spectra of control composite, Al_2O_3 -based composite, and CNC-based composite

Thermogravimetric Analysis (TGA)

The thermogravimetric analysis (TGA) of the control, Al_2O_3 -based, and nanocellulose-incorporated composites revealed distinct differences in their thermal stability and degradation behavior (Figure 5). The control composite exhibited the highest overall weight loss (98.98%), indicating relatively poor thermal stability. Its minimal residue content (1.02%) suggests that the composite consisted predominantly of thermally labile organic matter, with limited non-volatile or thermally stable phases. In contrast, the Al_2O_3 -based composite showed improved thermal stability, with a total weight loss of 92.3% and a higher residual content of 7.7%. The greater residue indicates the presence of thermally stable inorganic constituents, particularly Al_2O_3 , which remained unaffected at elevated temperatures. This suggests that incorporating Al_2O_3 enhanced the composite's resistance to thermal decomposition compared to the control. The nanocellulose-reinforced composite demonstrated further improvement in thermal behavior compared to the control, but slightly lower stability than the Al_2O_3 -only system. The total weight loss was 94.92%, leaving 5.09% residue. While the introduction of nanocellulose increased the organic content, which decomposed, it also enhanced structural reinforcement and thermal resistance relative to the control composite. The higher char residue compared to the control indicates the beneficial role of Al_2O_3 , while the slightly reduced residue compared to the Al_2O_3 -only composite reflects the partial degradation of nanocellulose. Differential thermogravimetric (DTG) analysis provided further insight into the degradation process. The control composite displayed a single sharp degradation peak at around 365 °C, corresponding to the breakdown of collagen and PVC chains, which underscores

its limited thermal stability. The Al_2O_3 -containing composite exhibited a broader and slightly shifted degradation peak toward higher temperatures (~372 °C), along with a reduced peak intensity, indicating delayed and more gradual weight loss due to the protective role of Al_2O_3. The CNC-reinforced composite showed degradation near 380 °C associated with nanocellulose decomposition and fiber breakdown. Thus, the hybrid system combined the thermal stability imparted by Al_2O_3 with the reinforcing capacity of nanocellulose, yielding a composite that balances thermal resistance with structural performance.

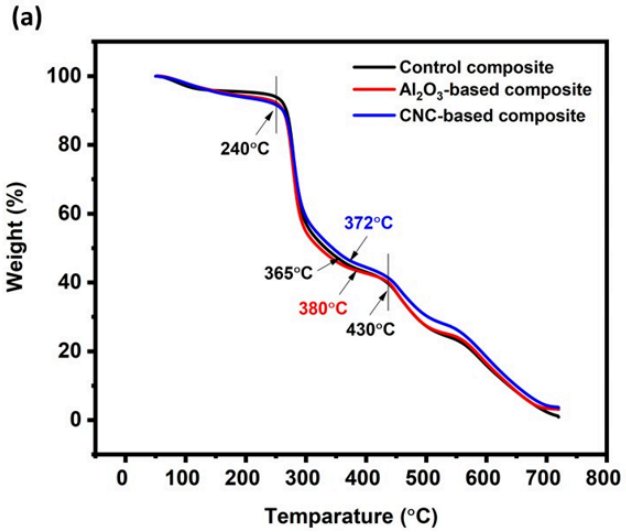

Figure 5. (a) TGA thermogram of composites with (b) derivatives

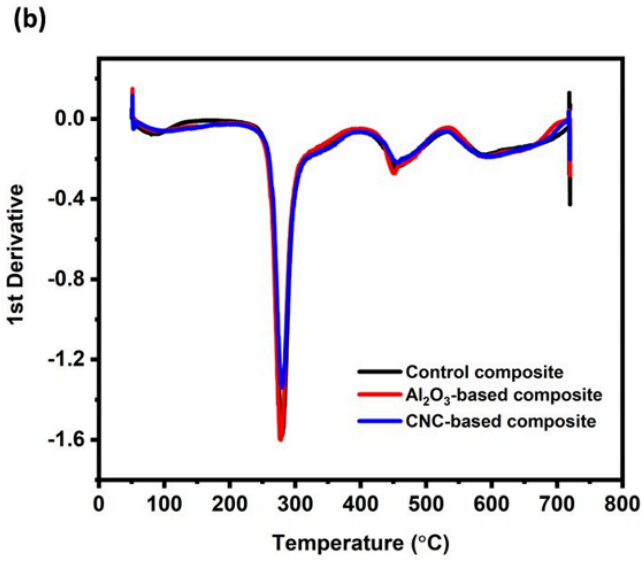

Figure 5. (a) TGA thermogram of composites with (b) derivatives

X-ray Diffraction (XRD) analysis

X-ray diffraction (XRD) analysis was performed to determine the crystalline structure, phase purity, and average crystallite size of the extracted nanocellulose. The diffraction pattern exhibited three characteristic peaks at 2θ values of 15.66°, 22.65°, and 34.40°, corresponding to the (110), (002), and (004) crystallographic planes of native cellulose-I, the most thermodynamically stable polymorph of cellulose [29] (Figure 6). Among these, the most intense reflection at 22.65° (002 plane) represents the dominant alignment of cellulose chains and indicates a relatively ordered structure. The sharpness of this peak enabled the determination of the largest crystallite size, approximately 3.87 nm, suggesting effective preservation of crystalline domains during oxidation. The diffraction peak at 15.66° (110 plane) was broader and less intense, corresponding to a smaller crystallite size of 2.69 nm. This feature reflects less ordered regions of the cellulose microfibrils and possible overlap with amorphous contributions. Similarly, the weakest and broadest peak at 34.40° (004 plane) yielded the smallest crystallite size (1.44 nm), indicative of short-range crystalline order and higher structural disorder within certain domains [30]. Collectively, these findings confirm that the extracted material retains nanoscale crystalline features characteristic of cellulose-I.

To further assess of crystallinity, the Crystallinity Index (CI) was determined using the Segal method. By comparing the intensity of the main crystalline peak (I002 = 1676 cps at 22.65°) with the amorphous background intensity (I_{am} = 367 cps at 15.66°), the CI was calculated as 78.07%. This relatively high crystallinity indicates that a substantial portion of the cellulose chains remained ordered even after nanoscale processing. The semi-crystalline nature of the nanocellulose, characterized by ordered crystalline domains interspersed with amorphous regions, is advantageous for composite applications, as it offers a balance between mechanical reinforcement (from the crystalline fraction) and flexibility or processability (from the amorphous fraction). The calculated crystallite size range of 1.44–3.87 nm further verifies the nanoscale reduction of cellulose fibrils while maintaining their essential crystalline architecture. Overall, these XRD results confirm the successful synthesis of nanocellulose with preserved structural integrity, high crystallinity, and nanoscale crystallite dimensions, making it a promising candidate for bio-based composite development and sustainable material applications where strength, flexibility, and compatibility with polymer matrices are critical.

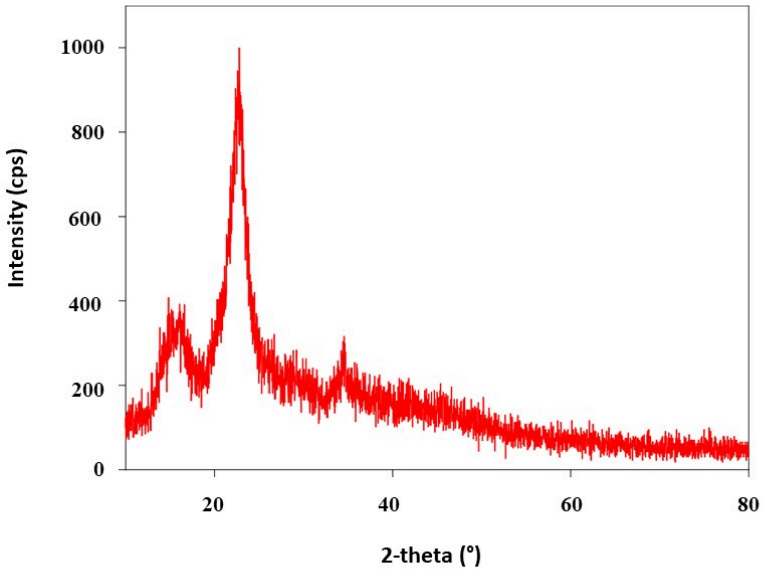

Figure 6. XRD pattern of the CNC-reinforced composite

FESEM analysis

The FESEM micrographs, captured at magnifications ranging from 5,000x to 30,000x using a secondary electron (SE2) detector at an accelerating voltage of 10.00 kV, provide valuable insights into the surface morphology of the nanocellulose-reinforced composite (Figure 7). The images reveal a porous and fibrous network typical of well-developed nanocellulose structures. The CNC fiber diameters ranged from 42 to 98 nm, confirming the nanoscale distribution and uniformity of the fibrillar network. The micrograph clearly shows a web-like, interconnected morphology, indicating that the cellulose nanofibers are well dispersed throughout the composite matrix. The observed morphology highlights the structural advantages of nanocellulose. Owing to their high aspect ratio and large specific surface area, the nanofibers establish extensive physical interactions with the surrounding matrix. Their strong intermolecular hydrogen bonding enables the formation of a continuous reinforcing network, thereby enhancing stress transfer, mechanical strength, and dimensional stability. Importantly, the absence of significant agglomeration or clustering in the FESEM images indicates effective dispersion and good interfacial compatibility, both critical for achieving homogeneity within the composite.

FESEM analysis confirms the successful incorporation of nanocellulose into the composite, yielding a porous, interconnected, and uniformly distributed fibrillar structure. This morphology not only underpins improved mechanical reinforcement and flexibility but also positions the material as a promising sustainable alternative for applications such as leather board production, reported previously by researchers [31].

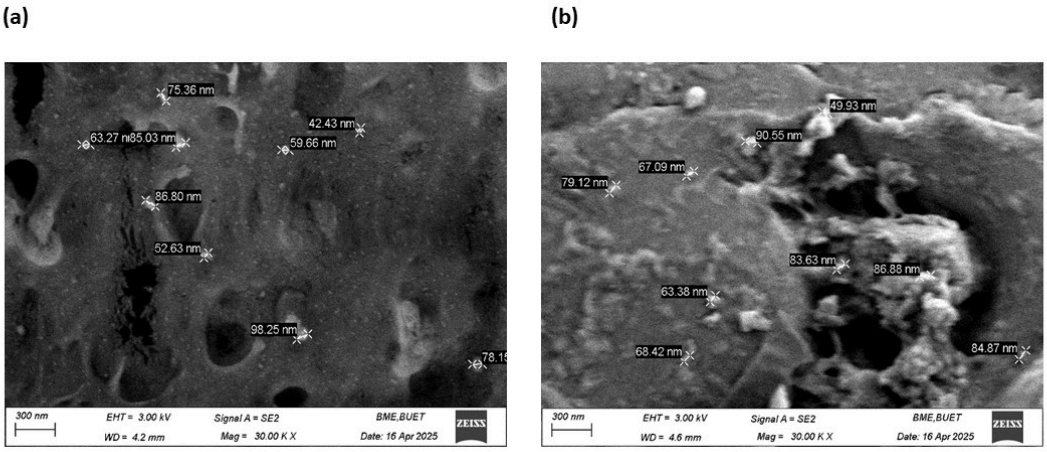

Figure 7. FESEM micrographs of the CNC-composite

Energy Dispersive X-ray Spectroscopy (EDS) analysis

Energy Dispersive X-ray Spectroscopy (EDS) was conducted to assess the elemental composition of the composite, which revealed that carbon (C) and oxygen (O) were the predominant elements, with normalized mass percentages of 61.01% and 37.05%, respectively (Figure 8b). The high carbon content reflects the organic constituents of the PVC matrix, leather powder, and CNC, whereas the oxygen content is associated with hydroxyl and carboxyl functional groups originating from CNC, as well as potential surface oxidation of leather and Al_2O_3 particles.

Minor elemental contributions were also identified. Chlorine (Cl), detected at 1.27%, corresponds to the chlorine backbone of PVC, confirming its incorporation into the composite matrix. Aluminum (Al) at 0.31% validates the successful integration of Al_2O_3 particles. A small sulfur (S) signal (0.36%) is likely derived from tanning agents or residual processing chemicals in the leather waste. Importantly, chromium (Cr), typically

associated with conventional chrome tanning, was absent, indicating that the leather powder used was either chrome-free or effectively purified prior to composite fabrication. EDS results confirm the incorporation of CNC and Al_2O_3 within the PVC-leather matrix. The observed elemental composition highlights the synergistic integration of organic and inorganic components, which is expected to enhance interfacial bonding, improve structural reinforcement, and improve the functional performance of the developed composite [32].

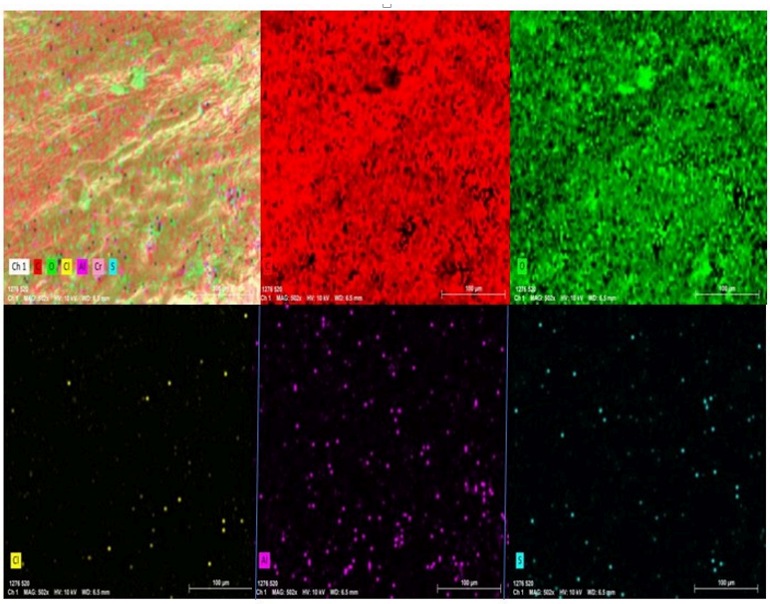

Figure 8a. EDS spectrum of the CNC-reinforced composite

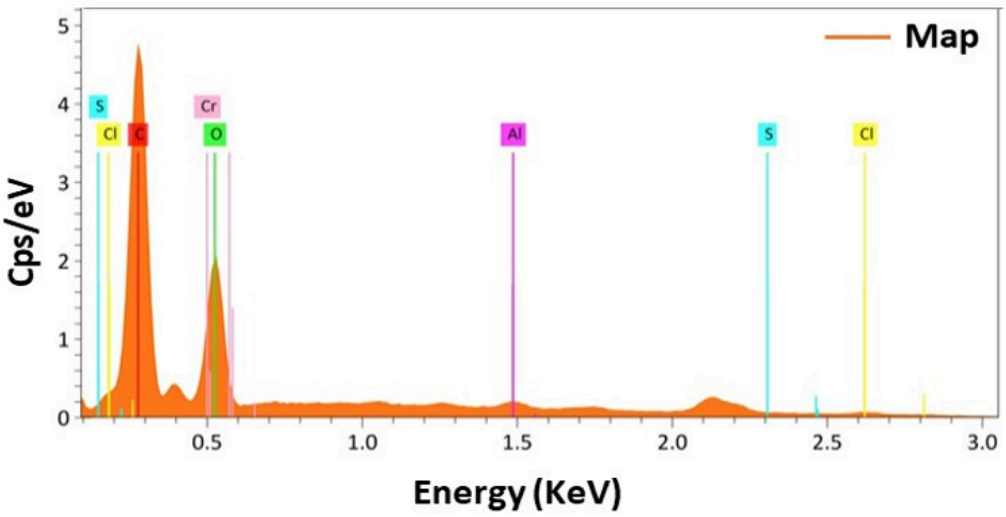

Figure 8b. EDS spectrum of the CNC-reinforced composite

Tensile strength

The incorporation of oxidized cellulose nanocrystals (CNC) markedly enhanced the tensile strength of the composites, particularly when combined with Al_2O_3 reinforcement (Table 5). The control sample, containing no fillers or CNC, exhibited the lowest tensile strength at 1.56±0.05 N/mm². The addition of Al_2O_3 alone significantly improved the strength to 2.80±0.04 N/mm², confirming its role as an effective reinforcing agent. Further improvements were observed with the inclusion of oxidized CNC. At 1% CNC loading, the tensile strength was 3.35±0.18 N/mm², increasing to 3.43±0.14 N/mm² at 3% CNC, representing the peak performance. A slight decline was observed at 4% CNC (3.40±0.17 N/mm²), likely due to nanofiller agglomeration at higher concentrations, which can hinder stress transfer efficiency. The enhanced tensile properties can be attributed to the synergistic reinforcement mechanisms of CNC and Al_2O_3. The oxidized CNC, with abundant hydroxyl and carboxyl groups, forms strong hydrogen bonds and interfacial interactions with the PVC–leather matrix, facilitating efficient stress transfer across the interface. Meanwhile, Al_2O_3 contributes through particle–matrix interlocking and the formation of rigid load-bearing sites, further restricting polymer chain mobility. At the optimal 3% CNC loading, these mechanisms operate synergistically, producing a well-dispersed reinforcing network that maximizes mechanical strength. In contrast, alternative fillers demonstrated limited reinforcement potential. $CaCO_3$ incorporation resulted in a tensile strength of only 1.92±0.06 N/mm², indicating poor compatibility with the composite matrix. ZnO provided moderate improvement, with a tensile strength of 2.46±0.06 N/mm², but did not match the reinforcing capability of CNC or Al_2O_3 . Overall, the combination of Al_2O_3 and 3% oxidized CNC produced the highest tensile strength (3.43±0.14 N/mm²), establishing CNC as a highly effective nanofiller for enhancing interfacial bonding, structural integrity, and load-bearing capacity in bio-based composites [19].

The maximum tensile strength of the nanocomposite developed in this study was 3.43 N/mm². This value is markedly higher than the previously reported range of 2.02–2.20 N/mm² [33]. The improvement is due to the reinforcing effect of cellulose nanocrystals from Nypa fruticans and the enhanced interfacial interactions within the PVC–leather matrix. A comparable tensile strength of 3.41 N/mm² was also reported for leather-based composites produced under different processes [34]. This further validates the reliability of the present findings.

Table 5. Tensile assessment of composites with different fillers and CNC loading

	Without CNC			With CNC incorporation			
	Force (N)	Area (mm ^{2})	Tensile strength	CNC %	Force (N)	Area (mm ^{2})	Tensile strength
Control	32.76±1.50	21±1.1	1.56±0.05	-	-	-	-
$CaCO_3$	44.16±1.79	23±1.2	1.92±0.06	-	-	-	-
ZnO	46.76±1.35	19±1.0	2.46±0.06	-	-	-	-
Al_2O_3	67.20±1.21	24±1.1	2.80±0.04	1	73.7±3.65	22±1.1	3.35±0.18
				3	82.3±4.11	24±1.1	3.43±0.14
				4	74.8±3.71	22±1.2	3.40±0.17

Elongation percentage

The mechanical performance of the composites, evaluated in terms of tensile strength and elongation, was strongly influenced by both filler type and the incorporation of cellulose nanocrystals (CNC). The control sample, prepared without CNC or reinforcing fillers, exhibited the lowest performance, requiring 32.76±1.50 N of force to break with an elongation at break of 21.67±1.08 mm (19.70±1.04%) (Table 6). The addition of Al_2O_3 alone considerably enhanced mechanical properties, increasing the breaking force to 67.20±1.21 N and elongation to 27.28±1.15 mm (24.80±1.13%), confirming its role as an effective reinforcing agent. Further improvement was achieved through the incorporation of CNC. At a 1% CNC loading, the composite exhibited a tensile strength of 73.7±3.65 N while retaining an elongation of 24.95±1.07%. At 3% CNC, the highest performance was recorded, with a tensile strength of 82.3±4.11 N and maximum elongation of 27.64±1.22 mm (25.13±1.11%), representing substantial gains in both strength and ductility. At higher loading (4% CNC), a slight reduction in tensile strength (74.8±3.71 N) and elongation (27.39±1.19 mm, 24.90±1.16%) was observed, likely due to nanofiller agglomeration, which can impede uniform stress distribution.

Comparative analysis with alternative fillers further highlights the superior reinforcing effect of CNC. Composites with $CaCO_3$ exhibited the poorest performance, with a breaking force of 44.16±1.79 N and an elongation of 25.98±1.30 mm (23.62±1.18%), indicating poor compatibility with the matrix. ZnO provided moderate reinforcement, achieving 46.76±1.35 N of tensile strength and 26.36±1.32 mm elongation (23.96±1.20%), though still inferior to Al_2O_3 or CNC-filled systems. The combination of Al_2O_3 and 3% CNC produced the greatest improvement in mechanical performance, delivering optimal strength and flexibility. These results highlight the synergistic effect of CNC and Al_2O_3 in improving interfacial bonding, stress transfer, and structural homogeneity, making the composite a strong candidate for high-performance, sustainable material applications.

The synthesized composite showed a higher average elongation at break than values reported in previous studies (17.75% [13] and 20.32% [35]), but a lower value than that reported in other studies on waste leather composites (31.4% [36] and 30% [6]). This pattern indicates that while the present composite demonstrates better flexibility than some reported systems, it remains less ductile than others. These differences are likely attributable to variations in filler content, dispersion quality, and matrix–filler interactions, which can affect elongation properties across the comparisons.

Table 6. Comparison of elongation at break values of synthesized composites

	Without CNC			With CNC incorporation			
	Force (N)	Extension at break (mm)	Elongation %	CNC %	Force (N)	Extension at break (mm)	Elongation %
Control	32.76±1.50	21.67±1.08	19.70±1.04	-	-	-	-
$CaCO_3$	44.16±1.79	25.98±1.30	23.62±1.18	-	-	-	-
ZnO	46.76±1.35	26.36±1.32	23.96±1.20	-	-	-	-
Al_2O_3	67.20±1.21	27.28±1.15	24.80±1.13	1	73.7±3.65	27.45±1.10	24.95±1.07
				3	82.3±4.11	27.64±1.22	25.13±1.11
				4	74.8±3.71	27.39±1.19	24.90±1.16

Water absorption

The water absorption behavior of the prepared leather composite sheets was evaluated to assess their resistance to moisture uptake, an important property influencing durability and dimensional stability. Test samples were immersed in water for a specified period, and the water uptake was measured one minute after drainage, with the percentage absorption calculated based on mass. The control composite exhibited a water absorption of 20.84%. Incorporation of Al_2O_3 increased the water uptake to 29.35%, which may be attributed to the hygroscopic nature of the filler and the creation of microvoids within the matrix that facilitate water penetration. The results also surpass the previously reported data [6]. In contrast, the addition of 3% cellulose nanocrystals (CNC) to the Al_2O_3 -based composite reduced water absorption to 19.63%, slightly lower than that of the control. This decrease indicates that CNC effectively reinforces the matrix, enhancing fiber–matrix interactions and reducing microvoids and porosity, thereby limiting water ingress.

These results demonstrate that while Al_2O_3 alone can increase hydrophilicity due to filler characteristics, the synergistic inclusion of CNC mitigates moisture absorption by forming a more compact and well-integrated network. Consequently, the 3% CNC-reinforced Al_2O_3 composite exhibits superior water resistance, high-

lighting the role of CNC in improving both the mechanical integrity and moisture durability of leather-based composites.

Implications of the Study

The results of this study enhance theoretical understanding of bio-nanocomposite design by illustrating the influence of the nanoscale structure, crystallinity, and surface chemistry of cellulose nanocrystals (CNC) on macroscopic performance in hybrid polymer systems. The increases in tensile strength, elongation, and thermal stability demonstrate the importance of hydrogen bonding at the interface and of synergistic reinforcement between bio-based and inorganic fillers. This offers a novel framework for elucidating the optimization of stress transmission and the limitation of polymer chain mobility in hybrid nanostructures integrating CNC and metal oxides, while maintaining flexibility. The structure–property connections developed in this study advance the overarching idea of sustainable composite mechanics by linking molecular interactions to overall performance. The research enhances scientific comprehension of *Nypa fruticans* as a cellulose source, providing novel insights into its crystallographic and morphological characteristics in the realm of green nanomaterials. This research offers a feasible method for upcycling two significant waste streams, such as leather scraps and agricultural biomass, into high-value, durable materials appropriate for the footwear and leather goods sectors. The optimized PVC–leather–CNC– Al_2O_3 composite is stronger, more flexible, and more stable than other materials. This makes it a good candidate to replace synthetic leather in shoe uppers, insole boards, and other performance applications. The method promotes the goals of a circular economy by turning garbage into useful composites. It also reduces pollution and creates jobs in sustainable manufacturing. This effort turns environmental problems into real technical and business solutions, bringing together scientific progress with global ambitions for sustainability.

CONCLUSION

The effective extraction of cellulose nanocrystals (CNC) from *Nypa fruticans* and their use in PVC–leather scrap composites signifies a notable development in sustainable material design. The isolated CNC had nanoscale dimensions (about 100 nm) and a high crystallinity (78.07%), which ensured that it worked well as a reinforcement in the polymeric matrix. FTIR and XRD tests showed that hemicellulose and lignin were removed while the cellulose-I structure stayed the same. FESEM images showed a homogeneous fibrillar network, contributing to robust interfacial adhesion. These traits made CNC a good nanofiller that can improve stress transfer and compatibility in hybrid composites. A couple of PVA-leather waste bio-composite sheets

were prepared at different ratios using Al_2O_3, $CaCO_3$, and ZnO as reinforcement materials. Among them, Al_2O_3 gives better results, and CNC was additionally introduced into the PVA-leather-Al_2O_3 composite sheet to increase its physio-mechanical properties. Mechanical tests indicated that adding CNC to the composite made it much stronger and tougher. With 3% CNC loading, the tensile strength went up to 3.43±0.14 N/mm², which is significantly higher than the control. The elongation at break increased to 25.13±1.11%, indicating a good balance of stiffness and flexibility. The synergy between CNC and Al_2O_3 nanoparticles was pivotal: CNC supplied hydrogen bonding and structural stability, while Al_2O_3 operated as rigid anchors that prevented polymer mobility and distributed stress. After 3% CNC, a slight drop in performance was attributed to nanoparticle aggregation, a normal saturation effect. Thermogravimetric studies confirmed improved thermal stability, with degradation delayed to about 380 °C and residual char rising from 1.02% to 5.09%. This proves that the hybrid system acts as a protective barrier. Also, the absorbed water decreased to 19.63%, indicating a denser, more compact structure with fewer microvoids. The nanoscale morphology and interfacial chemistry of CNC provide mechanical reinforcement, while the inorganic phase adds thermal and dimensional stability. This work demonstrates that *Nypa fruticans* can be utilized as an innovative, sustainable source of CNC, while leather waste can be efficiently transformed into high-performance bio-nanocomposites. The optimized PVC–leather-CNC-Al_2O_3 composite is a better choice for making shoes and leather items because it is stronger, more flexible, and lasts longer, aligning environmental responsibility with industrial functionality. This dual-waste valorization pathway shows how the circular economy works by promoting both new materials and protecting the environment. Overall, this research not only contributes to the theoretical understanding of the reinforcement mechanisms of bio-nanocomposites but also provides a practical solution to advance circular economy principles.

Author Contributions

Md. Ariful Islam: Writing original draft, visualization, review; Nujhat Tabassum; Experimental work, formal analysis, investigation, data collection, visualization; Md. Abdus Shabur; Review and editing; Umme Habiba Bodrun Naher: Revision, writing, and Review; Md. Abdul Mottalib: conceptualization, investigation, methodology, review, and supervision. All authors have read and agreed to the published version of the manuscript.

Conflicts of Interest

The authors declare no conflict of interest.

Funding

This research received no external funding.

Acknowledgements

The authors gratefully acknowledge the Institute of Leather Engineering and Technology, University of Dhaka for providing all kinds of supports to carry out this research.

REFERENCES

[1] Ncube A, Fiorentino G, Panfilo C, De Falco M, Ulgiati S. Circular economy paths in the olive oil industry: a Life Cycle Assessment look into environmental performance and benefits. International Journal of Life Cycle Assessment 2024; 29:1541-61. doi: 10.1007/s11367-022-02031-2

[2] Ramamurthy G, Ramalingam B, Katheem MF, Sastry TP, Inbasekaran S, Thanveer V, Jayaramachandran S, Das SK, Mandal AB. Total Elimination of Polluting Chrome Shavings, Chrome, and Dye Exhaust Liquors of Tannery by a Method Using Keratin Hydrolysate. ACS Sustain Chem Eng 2015; 3:1348-58. doi: 10.1021/acssuschemeng.5b00071

[3] Zottin LS. The environmental performance of footwear in an eco-friendly company and recommendations to increase sustainable value creation. 2019. Master Thesis_Ligia Zottin_5965020.

[4] Fatema K, Sarker MR, Akhtar K, Begum A, Islam S. Environmental sustainability: a challenge for leather industry. Leather and Footwear Journal 2023; 23:209-26. doi: 10.24264/lfj.23.3.6

[5] Alemu LG, Kefale GY, Hailu R, Tilahun A, Minbale E, Eyasu A. Toward Sustainable Leather Processing: A Comprehensive Review of Cleaner Production Strategies and Environmental Impacts. Advances in Materials Science and Engineering 2024; 2024. doi: 10.1155/2024/8117915

[6] Islam MA, Haque P, Rahman MM. Development of latex-based sustainable composites reinforced with leather trimming dust and ZnO nanoparticles for antibacterial shoe insole application: A circularity approach. Circular Economy 2026; 5. doi: 10.1016/j.cec.2026.100181

[7] Thakur VK, SAS, & MIK. Renewable Resource-Based Green Polymer Composites: Analysis and Characterization. International Journal of Polymer Analysis and Characterization 2010; 15:137-46. doi: 10.1080/10236660903582233

[8] Saha B, & AFABin. Probable Ways of Tannery's Solid and Liquid Waste Management in Bangladesh - An Overview. Textile & Leather Review 2021; 4:76-95. doi: 10.31881/TLR.2020.25

[9] Shakil SR, Yeasmin MN, Asif SMR, Nila UH, Mottalib MA. Preparation and Characterization of Ethylene Vinyl Acetate-Based Composites from Footwear Scraps and Peanut Fiber for Value-Added Products. Fibers and Polymers 2025; 26:2159-74. doi: 10.1007/s12221-025-00943-y

[10] Owonubi SJ, Agwuncha SC, Malima NM, Shombe GB, Makhatha EM, Revaprasadu N. Non-woody Biomass as Sources of Nanocellulose Particles: A Review of Extraction Procedures. Front Energy Res. 2021;9. doi: 10.3389/fenrg.2021.608825

[11] Das PP, Chaudhary V. Environmental impact and effect of chemical treatment on bio fiber based polymer composites. Mater. Today Proc. 2020; 49:3418-22. doi: 10.1016/j.matpr.2021.03.097

[12] Chakma S, Fatama K, Akter N, Nur-E-Alam M. Textile & Leather Review Potential Utilization of Solid Wastes Generated from Tannery, Garments and Jute Industries for the Production of Composite Board n.d. doi: 10.31881/TLR.

[13] Tauhiduzzaman M, Mottalib MA, Rahman MJ, Kalam MA. Preparation and characterization of composite sheets from solid leather waste with plant fibers: a waste utilization effort. Clean Technol Environ Policy. 2024; 26:1025-38. doi: 10.1007/s10098-023-02642-9

[14] Aaliya B, Sunooj KV, Lackner M. Biopolymer composites: a review. International Journal of Biobased Plastics. 2021; 3:40-84. doi: 10.1080/24759651.2021.1881214

[15] Thooyavan Y, Kumaraswamidhas LA, Raj RE, Binoj JS. Influence of SiC micro and nano particles on tribological, water absorption and mechanical properties of basalt bidirectional mat/vinyl ester composites. Compos Sci Technol. 2022; 219:109210. doi: 10.1016/J.COMPSCITECH.2021.109210

[16] Sajin JB, Babu Aurtherson P, Binoj JS, Manikandan N, Senthil Saravanan MS, Haarison TM. Influence of fiber length on mechanical properties and microstructural analysis of jute fiber reinforced polymer composites. Mater Today Proc. 2021; 39:398-402. doi: 10.1016/J.MATPR.2020.07.623

[17] Parisi M, Nanni A, Colonna M. Recycling of chrome-tanned leather and its utilization as polymeric materials and in polymer-based composites: A review. Polymers (Basel). 2021; 13:1-23. doi: 10.3390/polym13030429

[18] Muralidharan V, Palanivel S, Balaraman M. Turning problem into possibility: A comprehensive review on leather solid waste intra-valorization attempts for leather processing. J Clean Prod. 2022; 367:133021. doi: 10.1016/J.JCLEPRO.2022.133021

[19] Tripathy SP, Mishra R, Dwivedi KK, Khathing DT, Ghosh S, Fink D. Proton induced modification in Poly(ethylene terephthalate). Radiation Effects and Defects in Solids. 2002; 157:1-11. doi: 10.1080/10420150214037

[20] Zhuang J, Li M, Pu Y, Ragauskas AJ, Yoo CG. Observation of potential contaminants in processed biomass using fourier transform infrared spectroscopy. Applied Sciences (Switzerland). 2020;10. doi: 10.3390/app10124345

[21] Mottalib MA, Adnan Z, Dhar MC, Tauhiduzzaman M, Shaikh MAA, Naim MR, Goni MA. Synthesis and characterization of nano-cellulose from Slender amaranth and its application as an eco-friendly reinforcement material

in synthetic leather preparation from leather scraps wastes. Polymer Bulletin. 2024; 81:9363-88. doi: 10.1007/s00289-024-05260-7

[22] Devnani GL, Sinha S. African Teff Straw as a Potential Reinforcement in Polymer Composites for Light-Weight Applications: Mechanical, Thermal, Physical, and Chemical Characterization before and after Alkali Treatment. Journal of Natural Fibers. 2020; 17:1011-25. doi: 10.1080/15440478.2018.1546640

[23] Rana MS, Rahim MA, Mosharraf MP, Tipu MFK, Chowdhury JA, Haque MR, Kabir S, Amran MS, Chowdhury AA. Morphological, Spectroscopic and Thermal Analysis of Cellulose Nanocrystals Extracted from Waste Jute Fiber by Acid Hydrolysis. Polymers (Basel). 2023;15. doi: 10.3390/polym15061530

[24] Nayak S, Khuntia S kumar. Development and study of properties of Moringa oleifera fruit fibers/ polyethylene terephthalate composites for packaging applications. Composites Communications. 2019; 15:113-9. doi: 10.1016/j.coco.2019.07.008

[25] Rashid ESA, Gul A, Yehya WAH, Julkapli NM. Physico-chemical characteristics of nanocellulose at the variation of catalytic hydrolysis process. Heliyon. 2021; 7:e07267. doi: 10.1016/J.HELIYON.2021.E07267

[26] Sun Y, Zhang H, Li Q, Vardhanabhuti B, Wan C. High lignin-containing nanocelluloses prepared via TEMPO-mediated oxidation and polyethylenimine functionalization for antioxidant and antibacterial applications. RSC Adv. 2022; 12:30030-40. doi: 10.1039/d2ra04152a

[27] Banerjee S, Ganguly S, Sen KK. Synthesis and biological evaluation of some novel triazole derivatives. Int J Pharm Appl. 2013:49-62.

[28] Ramlath K, Sajna P, Nusrath P, Rajesh C. Isolation and characterisation of cellulose fibre from pennisetum polystachion and its application in biocomposites with ethylene propylene diene monomer rubber. Cellulose Chem. Technol. 2023; 57.

[29] Salem KS, Kasera NK, Rahman MA, Jameel H, Habibi Y, Eichhorn SJ, French AD, Pal L, Lucia LA. Comparison and assessment of methods for cellulose crystallinity determination. Chem Soc Rev. 2023; 52:6417-46. doi: 10.1039/d2cs00569g

[30] Santmartí A, Lee K-Y. Crystallinity and thermal stability of nanocellulose. Nanocellulose and sustainability, CRC Press; 2018, p. 67-86.

[31] Amusa AA, Mohd Razali NI, Ali F, Tuan Ismail TNM, Azmi AS, Jamaluddin J. Optimization of microwave-assisted polycondensation for flexible biodegradable polyurethane in sustainable packaging applications. Mater Today Commun. 2025;44. doi: 10.1016/j.mtcomm.2025.111878

[32] Stotz HU, Findling S, Nukarinen E, Weckwerth W, Mueller MJ, Berger S. A tandem affinity purification tag of TGA2 for isolation of interacting proteins in Arabidopsis thaliana. Plant Signal Behav. 2014; 9:1-10. doi: 10.4161/15592316.2014.972794

[33] Teklay A. Solid Leather Waste for Preparation of Value Added Composite Products: An Ethiopian Perspective. 2021.

[34] Senthil R, Hemalatha T, Kumar BS, Uma TS, Das BN, Sastry TP. Recycling of finished leather wastes: A novel approach. Clean Technol Environ Policy. 2015; 17:187-97. doi: 10.1007/s10098-014-0776-x

[35] Teklay A, Gebeyehu G, Getachew T, Yaynshet T, Sastry TP. Preparation of value added composite boards using finished leather waste and plant fibers—a waste utilization effort in Ethiopia. Clean Technol Environ Policy. 2017; 19:1285-96. doi: 10.1007/s10098-016-1327-4

[36] Teklay A, Gebeyehu G, Getachew T, Yaynshet T, Inbasekaran S, Sastry TP. Preparation of value added composite sheet from solid waste leather-A prototype design. Scientific Research and Essays. 2018; 13:11-3.